Archives of Current Research International
6(3): 1-14, 2016; Article no.ACRI.30239
ISSN: 2454-7077

SCIENCEDOMAIN *international*
www.sciencedomain.org

Material Selection and Fluid Flow Analysis of Parallel Flow Heat Exchanger

Christian Emeka Okafor[1*], Alex Dubem Tagbo[2], Obiora Jeremiah Obiafudo[3] and Emmanuel Chinagorom Nwadike[1]

[1]Department of Mechanical Engineering, Nnamdi Azikiwe University, Awka, Nigeria.
[2]Institut fuer Energietechnik, Technische Universität Berlin, Fasanenstr, 89, 10623, Berlin, Germany.
[3]Department of Industrial/Production Engineering, Nnamdi Azikiwe University, Awka, Nigeria.

Authors' contributions

This work was carried out in collaboration between all authors. Author CEO designed the study, performed the statistical analysis, wrote the protocol, and wrote the first draft of the manuscript. Authors ADT and OJO managed the analyses of the study. Author ECN managed the literature searches. All authors read and approved the final manuscript.

Article Information

DOI: 10.9734/ACRI/2016/30239
Editor(s):
(1) R. M. Chandima Ratnayake, Department of Mechanical and Structural Engineering and Materials Science, University of Stavanger, Norway.
Reviewers:
(1) Fateh Mebarek-Oudina, Skikda University, Algeria.
(2) Mohammad Reza Safaei, University of Malaya, Malaysia.
(3) S. M. Arifuzzaman, Khulna University, Bangladesh.
Complete Peer review History: http://www.sciencedomain.org/review-history/17612

Original Research Article

Received 27th October 2016
Accepted 28th December 2016
Published 26th January 2017

ABSTRACT

Aims: To select appropriate material and undertake fluid flow analysis of parallel flow heat exchanger.
Methodology: Dynamic simulation study was performed to evaluate conditions of heat transfer of water through heat exchanger using ASPEN HYSYS. Cambridge Education Selector (CES) Granta software was used to select the suitable candidate materials for the heat exchanger. The properties of the selected materials and fluid characteristics were implemented in Computational Fluid Dynamics (CFD) to solve and analyze the fluid flow.
Results: For inner pipe, low alloy steel having maximum thermal conductivity of 55(W/m°C) and specific heat capacity of 530 (J/kg°C) respectively was selected and used. For the outer pipe, cast iron, gray having thermal conductivity of 72 (W/m°C) and specific heat capacity of 495(J/kg°C) passed the selection criteria and was used.The total heat transfer surface area and hydraulic

**Corresponding author: Email: ce.okafor@unizik.edu.ng;*

diameter was determined as 0.1341634m^2 and 0.481m respectively while the velocity of flow (V) for hot and cold fluid was established as 0.00014518 m/sec and 0.000196817 m/sec respectively.
Conclusion: The material-process decision on a parallel flow heat exchanger design was reduced to trade-off between performance and cost. The data obtained from the experimental record are well matched with computational fluid dynamics simulated values at different mass flow rate.

Keywords: Parallel flow; CFD; ASPEN HYSYS; Heat transfer; fluid flow.

1. INTRODUCTION

There have been reported cases of heat exchanger failure in service due to the extreme service conditions, such failure may have occurred due to poor material selection. Design is the process of translating a new idea or a market need into the detailed information from which a product can be manufactured, in addition, each state of design requires decision about the material of which the product is to be manufactured and the process involved in making it; normally, the choice of material is dictated by the design. The performance of an engineering component is therefore limited by the properties of the material of which it is made. Under some circumstances a material can be selected satisfactorily by specifying ranges for individual properties. More often, however, performance depends on a combination of properties, and then the best material is selected by maximising one or more performance indices [1].

A key element in the heat exchanger analysed in this study is the tube wall that separates two fluid streams (hot and cold) which travel in the same direction. The two streams enter at one end and leave at the other end [2]. Ali and Shaban [3] designed a heat exchanger to pasteurize milk by steam in a dairy plant and they did their calculation processes manually to specify the tube length and the number of tubes, and the pump for the heat exchanger. Osueke et al. [4] Experimentally investigated the effect of fluid flow rate on the performance of a parallel flow heat exchanger. Also Sivakumar and Rajan [5] undertook performance analysis of heat transfer and effectiveness on laminar flow with effect of various flow rates, the final point of their experimental assessment was validation with the numerical values. Araromi et al. [6] designed and developed a small heat exchanger as auxiliary cooling system for domestic and industrial applications. T'Joena et al., [7] reviewed polymer heat exchangers for HVAC&R applications and concluded that a successful application of polymers or polymer matrix composites are based on careful material selection and modification of the design to fully exploit the material properties.

Recently, the use of Computational Fluid Dynamics (CFD) to solve and analyze fluid flow has been advocated by researchers, Hesham [8] conducted experimental and CFD analysis of turbulent flow heat transfer in tubular exchanger. Ranjbar and Seyyedvalilu [9] reported a numerical investigation of the influence of different parameters such as coil radius, coil pitch and diameter of tube on the characteristics of heat transfer in helical double tube heat exchangers using the well-known Fluent CFD software. Reddy and Rao [10] designed and analysed the simulation reports of an existing heat exchanger, they utilised the material library of the Solid Works in attaining better knowledge related to properties of various materials for the heat exchanger. Marjan et al., [11] investigated heat transfer and pressure drop of a counter flow corrugated plate heat exchanger using MWCNT based nanofluids. Marjan et al., [12] investigated heat transfer performance and friction factor of a counter-flow double-pipe heat exchanger using nitrogen-doped, graphene-based nanofluids. One of the major limitations in the early heat exchangers was the poor performance of materials used in the high temperature high pressure areas of the heat exchanger. Consequently, the need for better materials to eliminate these flaws necessitated further research in the field of alloys and manufacturing.

2. MATERIALS AND METHODS

Cambridge Education Selector (CES) Granta software was used to select the suitable candidate materials for the heat exchanger. This was done by considering the function, objective and constraints of the heat exchanger as shown in Table 1. The constraints considered for the selected materials are cost and availability. Different material attributes like density, thermal conductivity and elastic limit were considered. Based on the function, objective and constraint, the material properties were plotted in bubble charts using Granta software and suitable candidate materials were selected.

Table 1. Design requirements for the heat exchanger

Function	Heat exchanger
Constraints	The wall thickness must be able to support pressure difference ∆p between the inside and outside Operating temperature up to 150^{o}C Modest cost
Objective	Maximize heat flow per unit area
Free variables	Tube wall thickness, t Material choice

2.1 Development of Equipment Performance Indices

Following Ashby [1] propositions, the flux into the tube wall by convention in W/m^2 is described by the heat transfer equation of (1).

$$q = h_1 \Delta T_1 \quad (1)$$

Where h_1 is the heat transfer coefficient and ΔT_1 is the temperature drop across the surface from fluid 1 into the wall. Conduction is described by the Fourier equation which is given as for one dimensional heat-flow

$$q = \lambda \frac{\Delta T_1}{t} \quad (2)$$

Where λ is the thermal conductivity of the wall (thickness t) and ΔT_1 is the temperature difference across it. One of the aims of this study is to select a material to maximize the total heat flow:

$$Q = qA = \frac{A\lambda}{t}\Delta T \quad (3)$$

Where $A = 2\pi rLn$ is the total surface area of the tube, this represents the objective function whereas the constraint is the wall thickness which must be sufficient to support the pressure difference between the inside and outside. This therefore requires that the stress in the wall remain below the elastic limit σ_y of the tube material multiplied by a safety factor

$$\sigma = \frac{r\Delta p}{t} < \sigma_y \quad (4)$$

This constrains the minimum value of t, hence eliminating t between equation 3 and 4 gives

$$Q = \frac{A\Delta T}{r\Delta p}(\lambda \sigma_y) \quad (5)$$

Following similar reasoning as in equations 1 to 5, the other indices and objective is shown in Table 2.

2.2 Test Procedure and Experimental Setup

The experimental setup for variable measurement and test trials is shown in Fig. 1. The fluid used are hot and cold water, parallel flow arrangement was implemented and trials were conducted with different mass flow rate of hot and cold water.

A dynamic simulation study was then performed to evaluate conditions of heat transfer of water through heat exchanger using ASPEN HYSYS. The cold water from the storage tank flows under gravity at temperature of 30^{O}C through a pump and an isolation valve into the heat exchanger, also the hot water temperature of 50^{O}C is passed through tube side of the heat exchanger. The experiment was repeated at different other hot and cold water flow rate without changing water tank temperature.

Table 2. The material indices and design objective

S/N	Material indices	Objective
1	$M_1 = \lambda \sigma_y$	Maximize heat flow per unit area of tube wall, Q/A
2	$M_2 = \frac{\lambda {\sigma_y}^2}{\rho}$	Maximize heat flow per unit mass of tube wall, Q/m
3	$M_3 = \frac{\lambda {\sigma_y}^2}{C_m \rho}$	Minimize cost per kg of the material

Where ρ = density of tube material, C_m = cost per kg of the material, σ_y is now raised to the power of 2 because the weight depends on wall thickness as well as density and wall thickness varies as $\frac{1}{\sigma_y}$

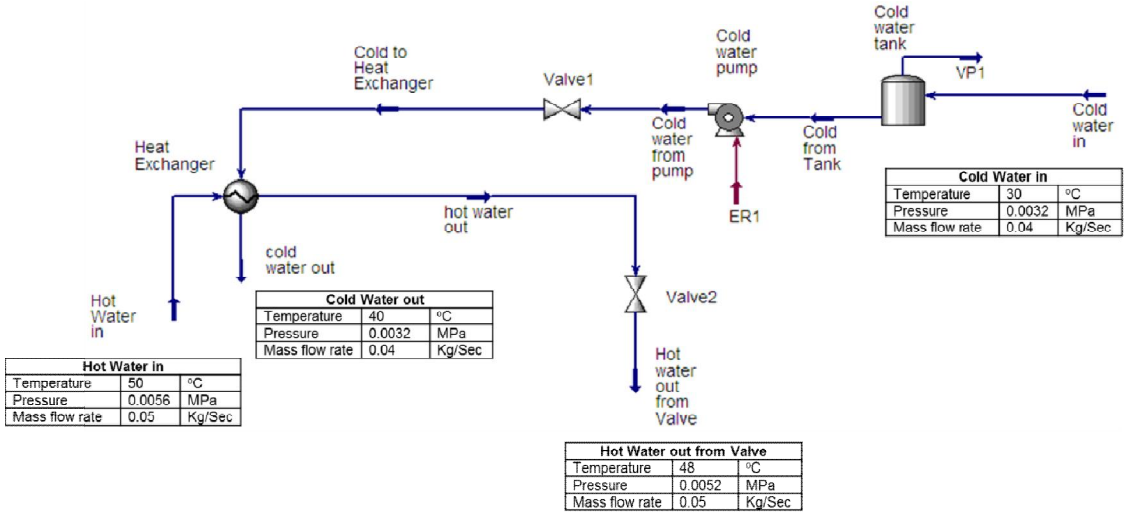

Fig. 1. Process flow diagram for variable measurement and test trials

Table 3. Fluid properties

S/N	Property	Unit	Cold water (30 °c)	Hot water (50°c)
1	Specific Heat (Cp)	kJ/kg. °C	4.174	4.174
2	Thermal conductivity (k)	W/m. K	0.6174	0.6526
3	Density (ϱ)	kg/m^3	996	988
4	Viscosity (Ω)	kg/m. s	0.00088	0.00086
5	Absolute Pressure	kN/m^2	3.2	5.6
6	Specific Entropy	kJ/KgK	0.505	0.367
7	Dynamic Viscosity μ	Kg/ms	0.000798	0.000547
8	Specific enthalpy of liquid water	kJ/kg	125.75	209.33
9	Kinematic viscosity	x10^{-6}m^2/s	0.8	0.553

Table 4. Heat exchanger data and details

S/N	Quantity	Symbol	Value	
			Inner pipe	Outer pipe
1	Tube inner diameter (m)	Dih	0.016	0.5
2	Tube outer diameter (m)	Doh	0.019	0.503
3	Tube length (m)	Lih	1.22	1.1
4	Thickness (mm)	Mm	1	1

2.3 Heat Exchanger Analysis

For design of a heat exchanger, it is necessary that the total heat transfer be related with its governing parameters such as the overall heat transfer coefficient due to various modes of heat transfer; total surface area of the heat transfer, and the inlet (t_1) and outlet (t_2) fluid temperatures. Let $\dot{m}$ = mass flow rate (kg/s); Cp = specific heat of fluid at constant pressure (J/kg°C); T = temperature of fluid (^{0}C); Δt = Temperature drop or rise of fluid across the heat exchanger (^{0}C).

Assuming that there is no heat loss to the surrounding and potential and kinetic energy changes are negligible; from the energy balance in a heat exchanger, Heat Duty (Q) (kW) is the capacity of the heat exchanger equipment expressed in terms of heat transfer per unit time [13].

Heat given up by the hot fluid

$$Q_h = \dot{m}_h c_{ph}(t_{h1} - t_{h2}) \quad (6)$$

Heat picked up (absorbed) by the cold fluid,

$$Q_c = \dot{m}_c c_{pc}(t_{c2} - t_{c1}) \quad (7)$$

Percentage (P) of losses or gains is

$$P = \frac{|Qc|}{|Qh|} \times 100 \quad (8)$$

$$\theta_m = \frac{\theta_2 - \theta_1}{ln(\theta_2/\theta_1)} = \frac{\theta_1 - \theta_2}{ln(\theta_1 - \theta_2)} \quad (9)$$

Total heat transfer rate in the parallel flow heat exchanger (Q) is given as

$$Q = UA\theta_m \quad (10)$$

U = overall heat transfer coefficient between the two fluids; A= effective heat transfer area, and θ_m = Appropriate mean value of temperature difference or logarithmic mean temperature (LMTD). The total heat transfer surface area is thus defined by Çengel [13] as

$$A_T = \frac{2\pi D_i L + 2\pi D_o L}{2} \quad (11)$$

Hydraulic diameter can be calculated with the generic equation proposed by Çengel [13] as

$$D_h = 4\frac{A}{p} \quad (12)$$

Where D_i and D_o are the inside and outside tube diameters, respectively and L is the tube length. D_h = hydraulic diameter (m); A = area section of the duct or pipe (m^2); p = "wetted" perimeter of the duct or pipe (m). Based on equation *(12)* the hydraulic diameter of a circular duct or tube with an inside duct or tube can be expressed as

$$D_h = 4\frac{(\pi r_o^2 - \pi r_i^2)}{(2\pi r_o - 2\pi r_i)} = 2(r_o - r_i) \quad (13)$$

Where: r_o = inside radius of the outside tube (m); r_i = outside radius of the inside tube (m)

$$Velocity\ of\ flow(V) = \frac{\dot{m}}{A\rho} \quad (14)$$

Where A = Area of flow in m^2; ρ = Density in kg/m^3 and $\dot{m}$= Mass flow rate in kg/sec.

2.4 Evaluation of System Fluid Flow Dimensionless Numbers and Physical Characteristics

2.4.1 The Reynolds number (Re)

The Reynolds number for internal flow is based on the internal diameter of the tube and the mean flow velocity over the tube across section:

$$R_e = \frac{inertia\ force}{viscous\ force} = \frac{\rho v D_H}{\mu} = \frac{V D_h}{v} \quad (15)$$

Where: V = mean velocity of the object relating to the fluid in m/s; D_h= Hydraulic Diameter in m; μ = dynamic viscosity of the fluid in kg/ms; *v* = Kinematic viscosity ($v = \frac{\mu}{\rho}$) in m^2/s; ρ = density of the fluid in kg/m^3

2.4.2 Prandtl number (Pr)

This is the ratio of momentum diffusivity (kinematic viscosity) to thermal conductivity.

$$P_r = \frac{Viscouse\ diffusion\ rate}{thermal\ diffusion\ rate} = \frac{v}{\alpha} = \frac{\mu C_p}{k} \quad (16)$$

$v =$ Kinematic viscosity (V) $= \frac{\mu}{\rho}$ (m^2/s) ;

$\alpha =$ Thermal diffusivity $= \frac{K}{\rho C_p}$ (m^2/s);

$\mu =$ Dynamic viscosity (Ns/m^2);

$C_p =$ Specific heat $\left(J/Kgk\right)$;

$k =$ Thermal Conductivity (W/mk);

$\rho =$ Density (Kg/m^3)

2.4.3 Nusselt Number (N_u)

Nusselt Number is the ratio of convective to conductive heat transfer across the boundary

$$N_u = \frac{hD_h}{K} \quad (17)$$

Where: h = Heat transfer coefficient; D_h = Hydraulic diameter in m; K = Thermal conductivity in W/Mk

2.4.4 Stanton number (S_t)

This is the ratio of Nusselt number and the product of Reynolds number and Pradndtl number.

$$S_t = \frac{N_u}{R_e \times P_r} \quad (18)$$

2.4.5 Peclet number (Pe)

This is the ratio of mass heat flow rate by convection to the flow rate by conduction under unit temperature gradient and through a thickness L

$$P_e = R_e \times P_r \quad (19)$$

2.4.6 The thermal efficiency of the heat exchanger (η)

In the parallel flow heat exchanger as depicted from the conceptual design (Fig. 1), some work is done to move the fluids over the heat transfer surfaces with the aid of a pumping system. Based on definition of the thermal efficiency (η), it is the ratio of the actual rate of heat transfer in a heat exchanger (Q) to the optimum rate of heat transfer (Q_{opt}):

$$\eta = \frac{Q}{Q_{opt}} = \frac{Q}{UA(\bar{T} - \bar{t})} \quad (20)$$

Where: $\bar{T}$= Average temperature of the hot fluid in °C, $\bar{T} = \frac{T_{h1}+T_{h2}}{2}$; $\bar{t}$ = Average temperature of the cold fluid in °C, $\bar{t} = \frac{t_{c1}+t_{c2}}{2}$; $U =$ Overall heat transfer coefficient in W/m^2 °C; $A =$ Heat exchanger surface area in m^2[14].

2.5 ANSYS Numerical Procedure

Procedure of numerical simulation of the parallel flow heat exchanger design is described in this section. Tetrahedral elements were used to discretize the domain, then linear unstructured mesh were generated by defining different curves and surfaces of the geometry, once a surface mesh is available, a volume mesh was then generated by filling the spaces between surfaces using tetrahedrons; Fig. 9 shows the refined FEM mesh used in the present study, the simulation was then ran for a computational time of nearly 30 minutes, which is sufficient to achieve steady state. the results obtained from the numerical model including the performance parameters are post-processed for better understanding and visualization of fundamental phenomenological behavior.

3. RESULTS AND DISCUSSION

Having carried out a search for materials that can suite the in-service condition of the parallel flow heat exchanger, the following materials presented in Table 5 met the search criteria as potential materials that can be used.

Each colour in Figs. 2-4 represents family of materials; the yellow colour code represent technical ceramics, the green colour represent foams, the pink colour represents metal and alloys and lavender colour represent composite materials. From the Figs. 2-4, and Table 5, it can be seen that a aluminum nitride stood out as good candidate for development of the inner tube of the parallel flow heat exchanger because of its low average density of 3295(kg/m^3) with a very high average thermal conductivity and specific heat capacity of 170(W/m.°C) and 800 (J/kg.°C) respectively. However due to its high cost, Low alloy steel having maximum thermal conductivity of 55(W/m.°C) and Specific heat capacity of 530 (J/kg.°C) respectively was selected and used [15]. For the outer pipe, cast iron, gray having thermal conductivity of 72 (W/m.°C) and specific heat capacity of 495(J/kg.°C) passed the selection criteria and was used. These choices are comparable to those made by Sivakumar and Rajan [5] in performance analysis of heat transfer and effectiveness on laminar flow with effect of various flow rates.

The total heat transfer surface area and hydraulic diameter has been determined from equation 11 and 12 as 0.1341634m^2 and 0.481m respectively while the velocity of flow (V) for hot and cold fluid was calculated using equation 14 as 0.00014518 m/sec and 0.000196817 m/sec respectively. The experimental results for cold and hot water are presented in Tables 6 and 7. From Tables 6 and 7, the range of values for the Reynolds number indicates that the flow characteristics of the heat exchanger studied is laminar in nature since *Re < 2300 [2; 13].*

Fig. 5 illustrates the exit hot fluid temperature with varying mass flow rate as measured from the heat exchanger. The validation took place with exit temperature of hot fluid of both experiment and simulation assessment. These values are in very good agreement with the simulated values.

Fig. 6 calibrated between the flow rate and overall heat transfer coefficient and the actual value is well validated with predicted value of simulation.

Figs. 7 and 8 showed the graph of hot and cold Reynold number against total heat transfer coefficient respectively. Reynolds number signifies the relative predominance of the inertia to the viscous force that occurred in the flow systems. The higher Re value recorded in the hot fluid section of the exchanger as shown in Fig. 7 signifies greater contribution of inertia effect, whereas the smaller Re value recorded in Fig. 8 signifies greater relative magnitude of the viscous stresses [2]. The simulated results are shown in Figs. 9-17.

Table 5. Values of material properties for the selected candidate materials

Materials	Density (kg/m^3)	Price (GBP/kg)	Young's modulus (GPa)	Yield strength (elastic limit) (MPa)	Maximum service temperature (°C)	Thermal conductivity (W/m.°C)	Specific heat capacity (J/kg.°C)	Thermal expansion coefficient (µstrain/°C)
Aluminum nitride	3.26e3-3.33e3	65.3-104	302-348	300-350	1.03e3-1.73e3	140-200	780-820	4.9-5.5
Low alloy steel	7.8e3-7.9e3	0.378-0.416	205-217	370-455	500-550	34-55	410-530	10.5-13.5
Medium carbon steel	7.8e3-7.9e3	0.353-0.39	200-216	305-900	-68.2- -33.2	45-55	440-520	10-14
Cast iron, gray	7.05e3-7.25e3	0.384-0.422	80-138	140-420	350-450	40-72	430-495	11-12.5
Low carbon steel	7.8e3-7.9e3	0.353-0.384	200-215	250-395	350-400	49-54	460-505	11.5-13

Table 6. Experimental results for cold water

S/N	mi_{tc}	Vc	Re_c	Nu_c	St_c	Pe_c
1	0.04	0.000299341	179.7083	1.583792654	1.633584	0.96952
2	0.05	0.000374177	224.6354	1.770734019	1.461122	1.2119
3	0.06	0.000449012	269.5624	1.939741931	1.333816	1.45428
4	0.07	0.000523847	314.4895	2.095160746	1.234873	1.69666
5	0.08	0.000598683	359.4166	2.239821052	1.155118	1.93904

Table 7. Experimental results for hot water

S/N	mi_{th}	Vh	Re_h	Nu_h	St_h	Pe_h
1	0.05	0.000374177	325.0808	1.846452897	1.623507	1.137323
2	0.06	0.000449012	390.0969	2.022687807	1.482053	1.364788
3	0.07	0.000523847	455.1131	2.184752531	1.372114	1.592253
4	0.08	0.000598683	520.1293	2.335598699	1.283495	1.819718
5	0.09	0.000673518	585.1454	2.477276518	1.210091	2.047182

Table 8. Results of hot and cold flow characteristics for the heat exchanger

mass frh (Kg/Sec)	mass frc (Kg/Sec)	Th1	Th2	Tc1	Tc2	Θ_m(^oC)	Q_h(J/sec)	Qc	Uh (W/m^2oC)	Uc ($W/m^{2o}C$)	U ($W/m^{2o}C$)	P
0.05	0.04	50	48	30	40	13.09628	417.4	1669.6	237.5584	950.2337	1187.792	400
0.06	0.05	50.3	49.4	30.6	40.5	13.5923	225.396	2066.13	123.6002	1133.002	1256.602	916.6667
0.07	0.06	50.7	50.3	30.7	40.6	14.23426	116.872	2479.356	61.19861	1298.285	1359.484	2121.429
0.08	0.07	51.9	51.1	30.7	40.9	15.03526	267.136	2980.236	132.4303	1477.426	1609.856	1115.625
0.09	0.08	52.5	51.4	30.8	41	15.36356	413.226	3405.984	200.4756	1652.405	1852.881	824.2424

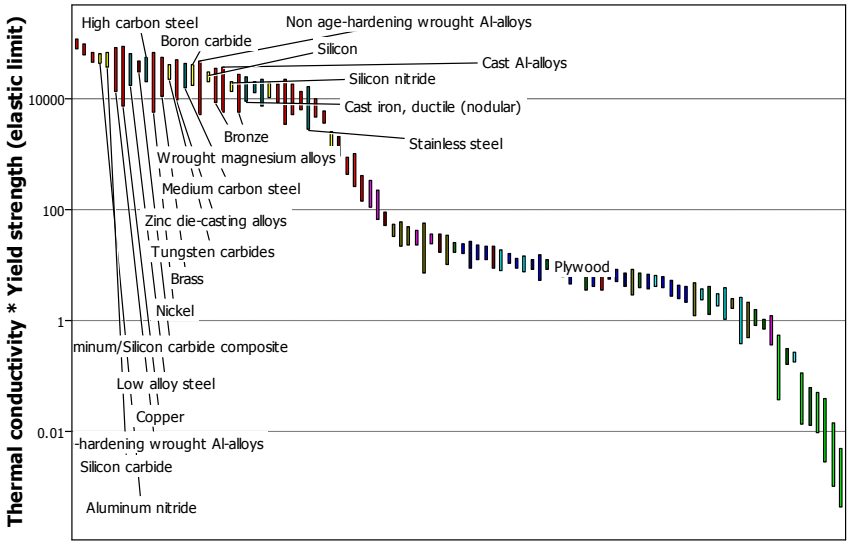

Fig. 2. Bubble chart of thermal conductivity and yield strength

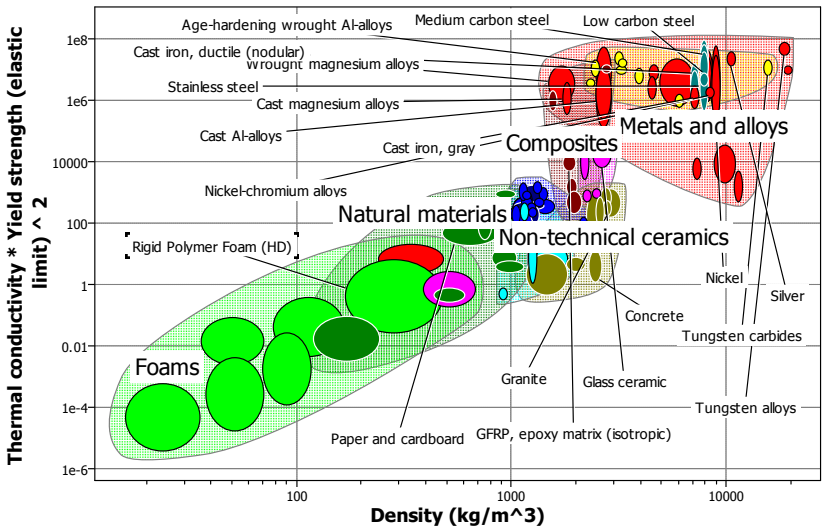

Fig. 3. Bubble chart of thermal conductivity*Yield strength against density

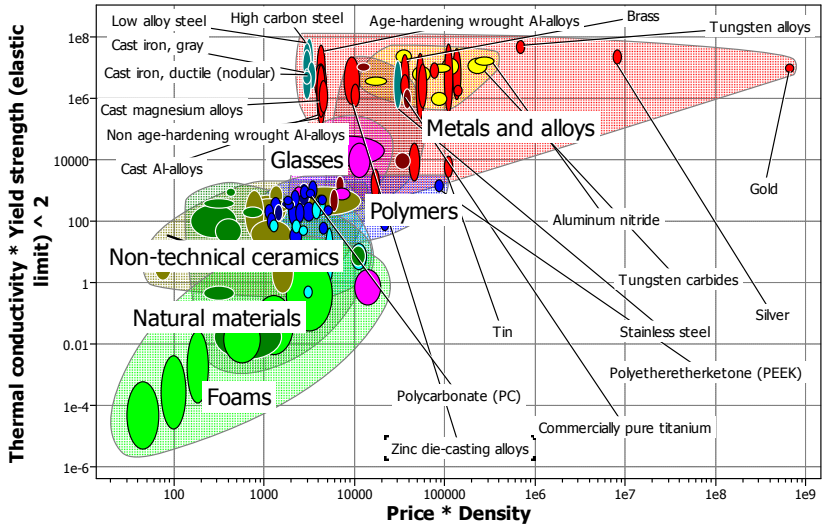

Fig. 4. Bubble chart of thermal conductivity* Yield strength against Price*Density

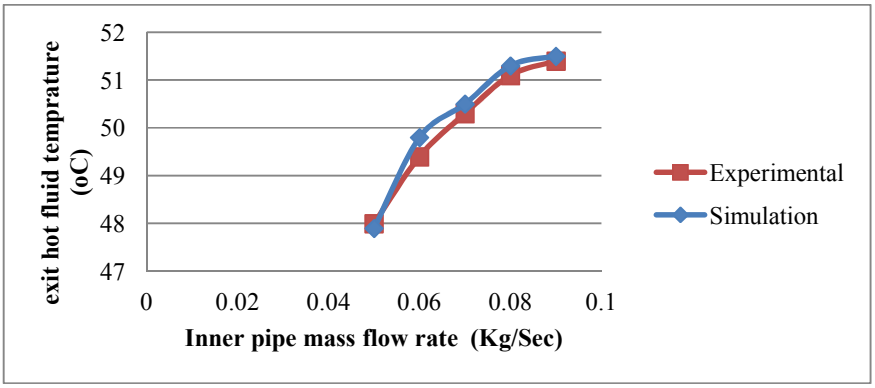

Fig. 5. Graph of exit hot fluid temperature versus inner pipe mass flow rate

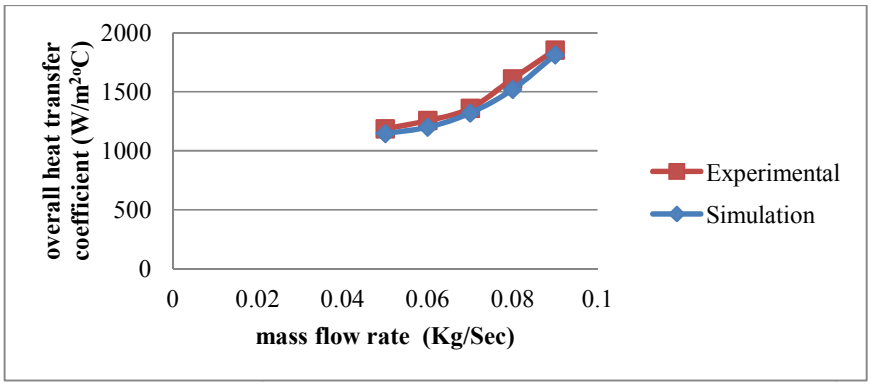

Fig. 6. Graph of overall heat transfer coefficient versus mass flow rate

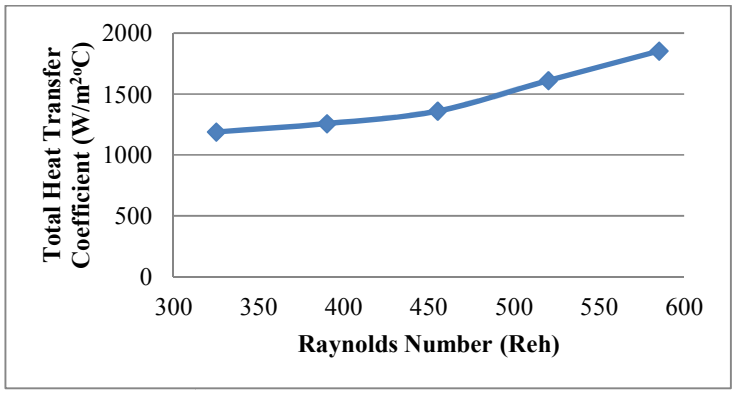

Fig. 7. Graph of hot Reynold number against total heat transfer coefficient

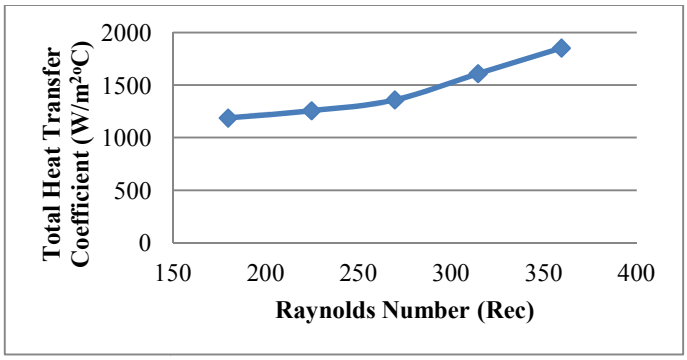

Fig. 8. Graph of cold Reynold number against total heat transfer coefficient

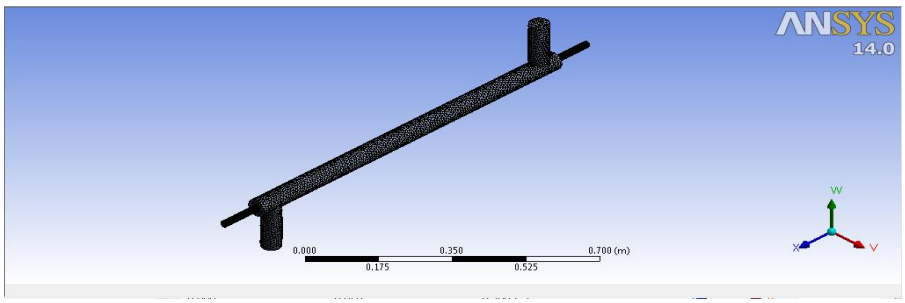

Fig. 9. Discretized parallel flow heat exchanger assembly

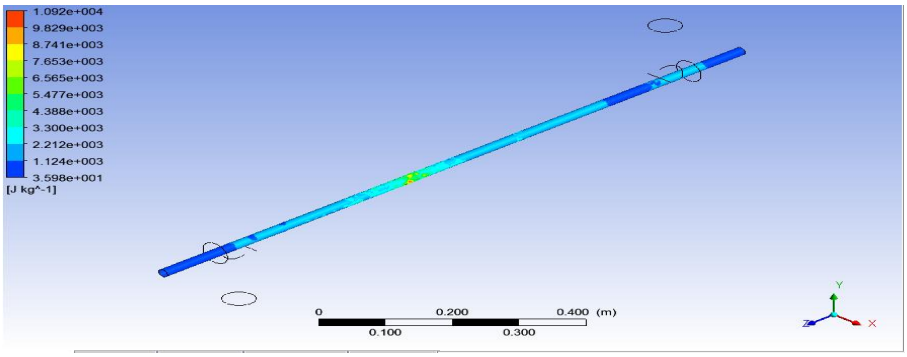

Fig. 10. Laminar Kinetic Energy contour for inner tube

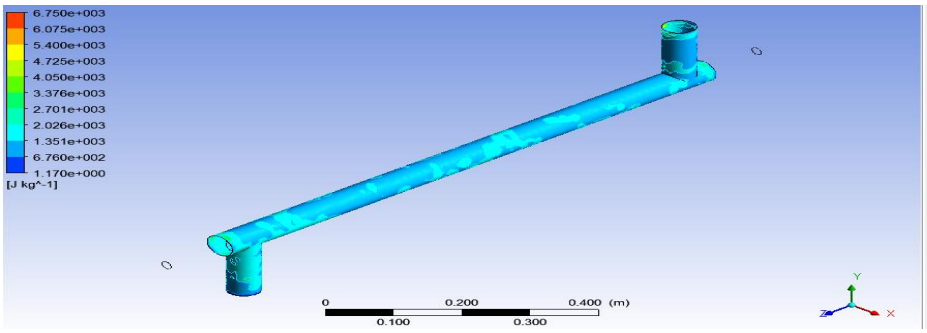

Fig. 11. Laminar kinetic energy for Outer tube

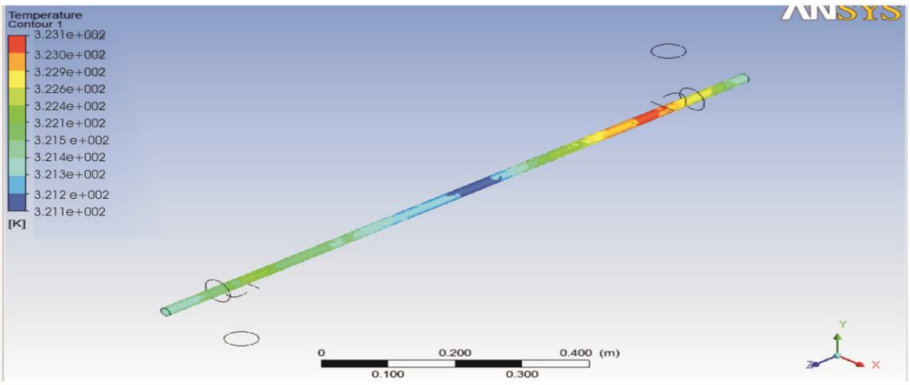

Fig. 12. Inner tube temperature distribution

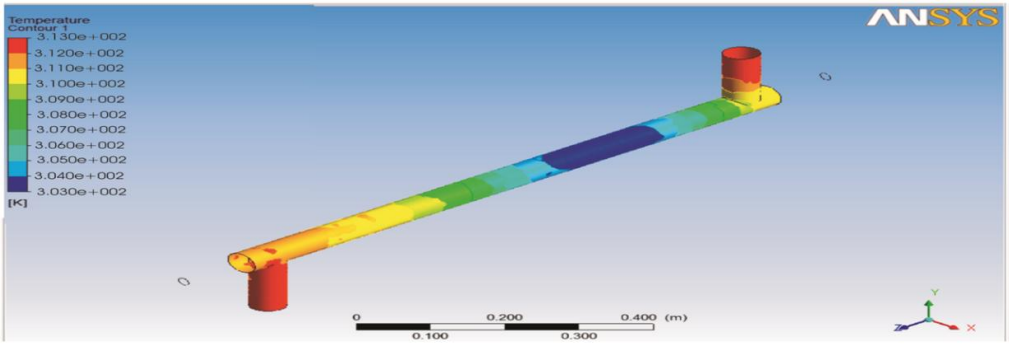

Fig. 13. Outer tube temperature distribution

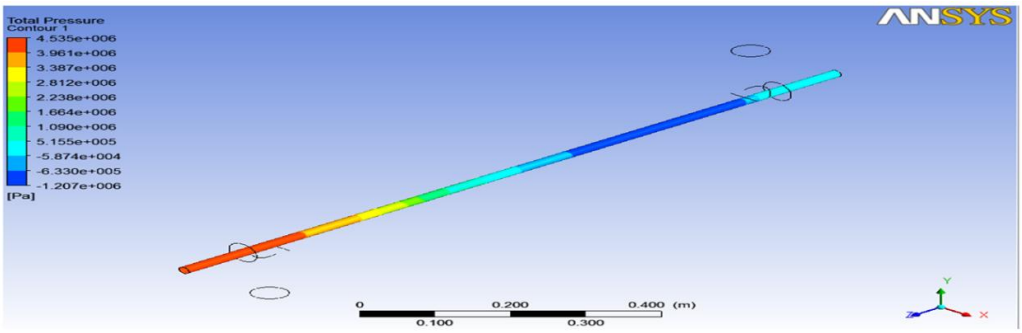

Fig. 14. Total pressure contour for the inner tube

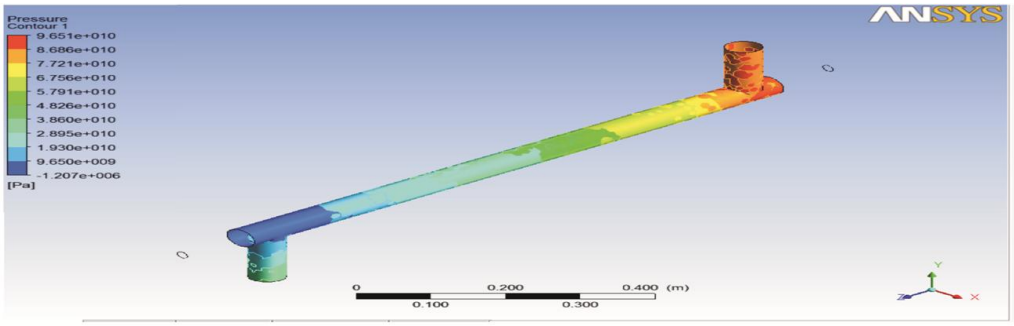

Fig. 15. Outer tube pressure distribution

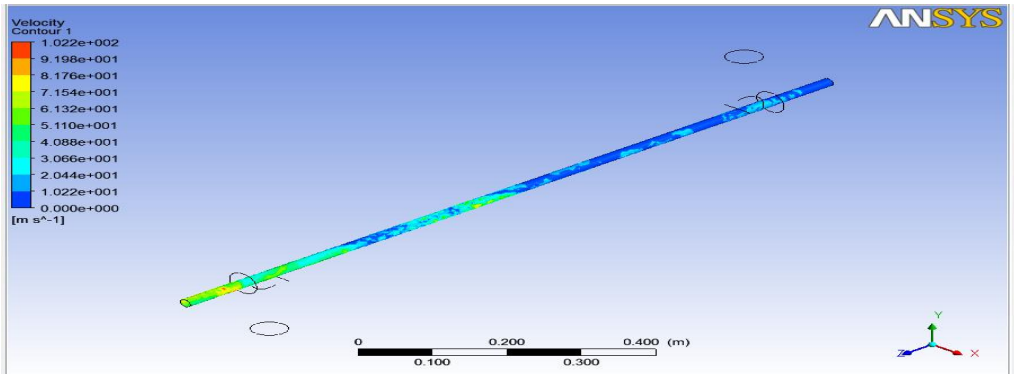

Fig. 16. Inner tube velocity distribution

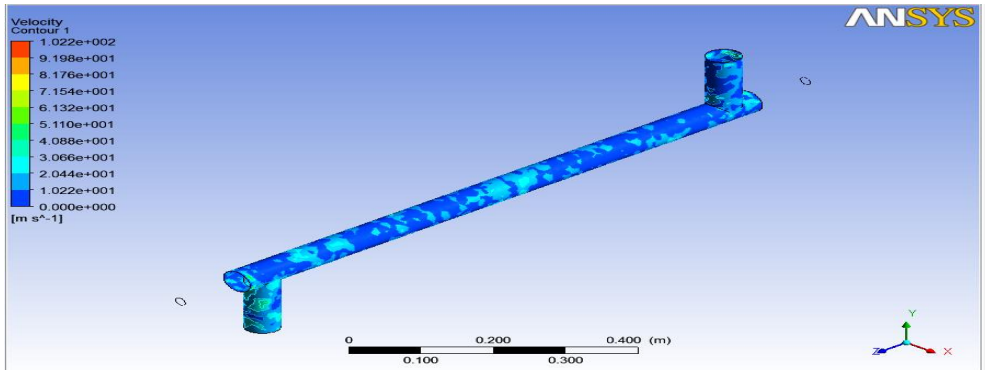

Fig. 17. Outer tube velocity distribution

Since it is not an irreversible problem, we are taking into consideration a one-dimensional parallel flow heat exchanger, whereby the equation 20 is applicable. For each mass flow rate level from the experiments conducted in Table 8, the following thermal efficiencies 0.93, 0.95, 0.96, 0.96 and 0.96 were calculated; hence, the average thermal efficiency is 0.95. This result is typically in agreement based on the availability of parameters. The actual performance can also be determined if expressions for the efficiency as a function of the system characteristics and operating conditions are known [16]. It can be suggested that the efficiency increases with increasing temperatures in a parallel flow heat exchanger. The tube wall thickness and the material choice for the design of the heat exchanger requirements, depend also on the operating inlet and exit temperature. Therefore, the future of this work will determine the sizing problems of a parallel flow heat exchanger under normal conditions.

4. CONCLUSION

The material-process decision on a parallel flow heat exchanger design was reduced to trade-off between performance and cost, in so doing, the study provided a value-to-cost ratio that is no worse and perfectly better than the competition, by value we mean the extent to which the performance criteria appropriate to the application are satisfied. The data obtained from the experimental record are well matched with computational fluid dynamics simulated values at different mass flow rate. Physical characteristics and thermal performance of a real heat exchanger were studied in this work.

COMPETING INTERESTS

Authors have declared that no competing interests exist.

REFERENCES

1. Ashby M. Materials selection in mechanical design. 4th Edition, Butterworth Heinemann; 2010.
2. Rajput RK. Heat and mass transfer. Second edition, New Delhi. S. Chand and company Ltd.; 2003.
3. Ali AL, Shaban A. Design of heat exchanger. Proceedings of the 2014 International Conference on Mechanics, Fluid Mechanics, Heat and Mass Transfer; 2014.
4. Osueke OC, Onokwai OA, Adeoye OA. Experimental investigation on the effect of fluid flow rate on the performance of a parallel flow heat exchanger. International Journal of Innovative Research in Advanced Engineering. 2015;6(2):10-23.
5. Sivakumar K, Rajan K. Performance analysis of heat transfer and effectiveness on laminar flow with effect of various flow rates. International Journal of Chem Tech Research. 2015;7(6):2580-2587.
6. Araromi OT, Oyelaran AO, Ogunleye LO. Design and development of a small heat exchanger as auxiliary cooling system for domestic and industrial applications. International Journal of Engineering Trends and Technology. 2013;5(6):314-319.
7. T'Joen C, Park Y, Wang Q, Sommers A, Han X, Jacobi A. A review on polymer heat exchangers for HVAC&R applications. International Journal of Refrigeration. 2009;32:763–779.
8. Hesham GI. Experimental and CFD analysis of turbulent flow heat transfer in tubular exchanger. International Journal of Engineering and Applied Sciences. 2014;5(7):17-24.
9. Ranjbar SF, Seyyedvalilu MH. The effect of geometrical parameters on heat transfer coefficient in helical double tube exchangers. Journal of Heat and Mass Transfer Research. 2014;1:75-82.
10. Reddy AS, Rao PS. Design and analysis based on the simulation reports of an existing heat exchanger. SSRG International Journal of Mechanical Engineering (SSRG-IJME). 2014;5:8-13.
11. Marjan G, Ahmad A, Mohammad SG, Mohammad RS, Arash K, Ehsan ML, Mahidzal D. Investigation of heat transfer and pressure drop of a counter flow corrugated plate heat exchanger using MWCNT based nanofluids. International Communications in Heat and Mass Transfer. 2015;66:172-179.
12. Marjan G, Kherbeet AS, Masoud A, Emad S, Mohammad M, Peyman Z, Somchai W, Daharih M. Investigation of heat transfer performance and friction factor of a counter-flow double-pipe heat exchanger using nitrogen-doped, graphene-based nanofluids. International Communications in Heat and Mass Transfer. 2016;76:16-23.
13. Çengel YA. Heat transfer: A practical approach. 2nd edition. Mcgraw-Hill; 2003.

14. Fakheri A. Heat exchanger efficiency. Journal of Heat Transfer. 2007;129:1268-1276.
15. Dieter G, Schmidt L. Engineering design 5th Edition, New York, NY 10020. Mcgraw-Hill Series in Mechanical Engineering; 2009.
16. Fakheri A. Efficiency analysis of heat exchangers and heat exchanger networks. International Journal of Heat and Mass Transfer. 2014;76:99-104.

Peer-review history:
The peer review history for this paper can be accessed here:
http://sciencedomain.org/review-history/17612